Hindawi Publishing Corporation
International Journal of Antennas and Propagation
Volume 2013, Article ID 279070, 7 pages
http://dx.doi.org/10.1155/2013/279070

Research Article

A New SVM-Based Modeling Method of Cabin Path Loss Prediction

Xiaonan Zhao, Chunping Hou, and Qing Wang

School of Electronics and Information Engineering, Tianjin University, Tianjin 300072, China

Correspondence should be addressed to Qing Wang; wqelaine@tju.edu.cn

Received 28 February 2013; Accepted 21 April 2013

Academic Editor: Yan Zhang

A new modeling method of cabin path loss prediction based on support vector machine (SVM) is proposed in this paper. The method is trained with the path loss values of measured points inside the cabin and can be used to predict the path loss values of the unmeasured points. The experimental results demonstrate that our modeling method is more accurate than the curve fitting method. This SVM-based path loss prediction method makes the prediction much easier and more accurate, which covers performance traditional methods in the channel propagation modeling.

1. Introduction

While wireless mobile communication is consolidated on the ground, it is still missing inside cabin during flight. This issue has recently been addressed to establish a wireless channel suitable for the cabin environment, which can meet the demand for wireless transmission at anywhere and anytime. For the special environment in cabin, it is necessary to take the modeling according to the actual measurement data due to the restriction of current indoor and outdoor channel model to the cabin's transmission environment. The path loss is one of the most important parameters to set up the channel model in the cabin environment. The state-of-art measurements of the path loss in large aircraft were mostly applied in narrow band and low-frequency band including 1.8 GHz, 2.1 GHz, and 2.4 GHz [1]. The measurement in high-frequency band was confined to the single-input single-output (SISO) system [2, 3]. The large-scale parameters (path loss, shadow fading, and seat penetration loss) and the small-scale parameters (fading distribution, typical K-factor values, and cabin wall penetration loss) and were related to the field strength [4, 5].

The theoretical prediction and field measurement are two different methods to obtain the radio propagation characteristics. The theoretical method, known as Computational Electromagnetic [6] based on the electromagnetic wave propagation theory, used the details of physical environment to make an accurate prediction. However, the calculation of cabin environment is limited by computation speed and memory size for the large and complex space of cabin. The field measurement, which needs to set the expensive and heavy equipment in the cabin, is limited by the narrow corridor space and the heavy equipment. Therefore, changing the cabin environment was proposed, and improved measurement results [7] were carried out with removing some seats inside the cabin (to change the original cabin interior environment). In this case, the accuracy of the models is critical.

The SVM, based on the statistical learning theory (SLT) and established on both the Vapnik Chervonenkis (VC) dimension theory and the minimum of the system risk [8], had a lot of applications in communication field recently [9, 10]. The optimal fitting between the complexity and the learning ability can be sought. A lot of problems, such as small sample, nonlinear and multiple dimensions, can be handled with SVM.

In this paper, for the first time, we predicted the path loss values based on SVM. Firstly, we measured path loss values of some selected points, then put the values in the model for training, and finally used the model to predict the values of unknown points. The B-spine surface fitting method was also adopted to compare with the SVM prediction.

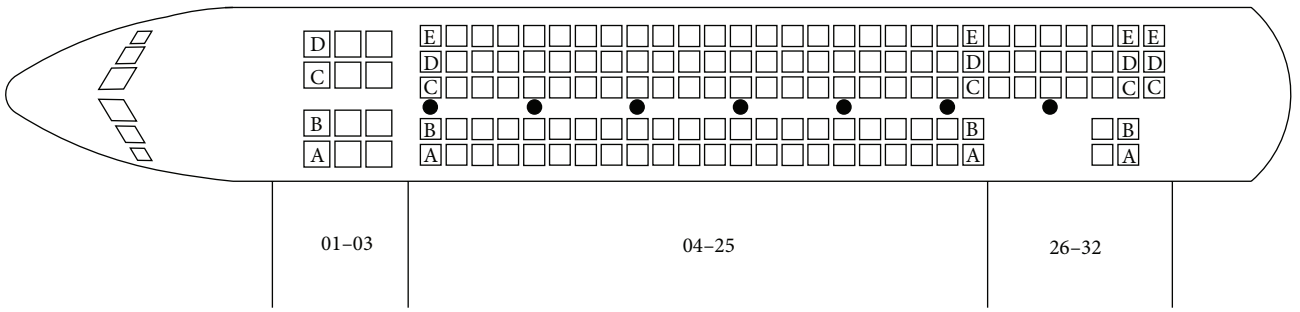

Figure 1: Cabin seat distribution.

This paper is organized as follows. Cabin interior measurements and path loss estimations is introduced in Section 2. The traditional surface fitting method for path loss forecasting is introduced in Section 3. The SVM-based path loss forecasting method is proposed in Section 4. Section 5 analyzes the path loss prediction in cabin using SVM and compares with the results achieved using surface fitting. Section 6 comes to the conclusion.

2. Cabin Interior Measurements and the Path Loss Calculation

The measurement equipment and data are provided by Tsinghua University, focusing on broadband (40 MHz bandwidth), distributed, and multiple antennas measurement. The equipment is a multiple-input single-output (MISO) system operating on 3.52 GHz. The measurement equipment is 3.52 Ghz MIMO radio channel sounder [11]. A lot of measurements have been done by students of Tsinghua University with the help of this equipment [12, 13]. The measurement is located in an MD82 commercial passenger aircraft. The transmitting node is equipped with distributed multiple antennas, while the receiving node with single antenna. This measure aims to analyze the field strength, large-scale, and small-scale parameters.

2.1. 3.52 GHz MISO Measurement Configurations. Transmitting terminal has seven 3.52 GHz distributed antennas on the top of cabin. Receiving terminal is a single fixed 3.52 GHz antenna. The transmitter power is 0 dBm, the gains of transmitting and receiving antenna are 4 dbi.

Two different locations of the receiving antenna are chosen to carry out the MISO measurement: fixed point of seat back and tables behind seat back. The two positions represent two main activities of the passengers: phone call and network access with laptops. The details of these two configurations are as follows.

(i) Scenario 1: fixed point of seat back: the height of seat back is 107.7 cm, and the width is 36.5 cm. The receiving antenna is placed in the middle of the seat back and stays vertical.

(ii) Scenario 2: fixed point of tables behind seat back: the height of the table is 61 cm, and the length is 42 cm. Similar to the fixed point measurement of seat back, the receiving antenna is placed in the middle of the table, to keep the antenna vertical.

In the economy class, fixed point measurements are carried out on the seat back and the table of seat. 22 rows from row 4 to row 25 are measured in economy class totally. The 4th to the 25th rows have five seats, marked as A, B, C, D, and E. The rest of the seats were not measured in this study. Black dot represents distributed antenna position. The cabin seat distribution is shown in Figure 1.

2.2. MISO Path Loss Calculation

Step 1. Using the matrix of channel impulse response, we can compute instantaneous power firstly:

$$P(t,\tau,s,u,p) = \left|h(t,\tau,s,u,p)\right|^2, \tag{1}$$

where t is the time, τ is the delay, s is the parameter of the transmitting antenna, u is the parameter of the receiving antenna, p is the power, and h is channel impulse response.

Step 2. Average the instantaneous power in transmitting and receiving antennas:

$$P(t,\tau,p) = \frac{1}{N_s N_u}\sum_{s=1}^{N_s}\sum_{u=1}^{N_u} P(t,\tau,s,u,p). \tag{2}$$

Step 3. Average the instantaneous power in Snap-dimensional and t-dimension:

$$P(\tau,p) = \frac{1}{n_t}\sum_{i=1}^{nt} P(t,\tau,p). \tag{3}$$

Step 4. Sum all clusters of the instantaneous power delay:

$$P(\tau,p) = \sum_{i=1}^{N_t} P(\tau,p). \tag{4}$$

Step 5. Match the receiving power P and the transmitting distance:

$$P(p) \longrightarrow P(d,p). \tag{5}$$

Step 6. Calculate the path loss PL of each link:

$$\mathrm{PL}(d,p) = P_{T_x}(d,p) + \sum_i Gi - \sum_i Ai - P(d,p), \tag{6}$$

where Gi is the gain of the antenna, Ai is the line attenuation.

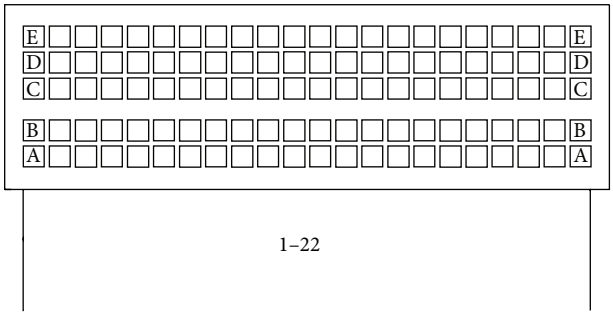

Figure 2: Renumbered rows.

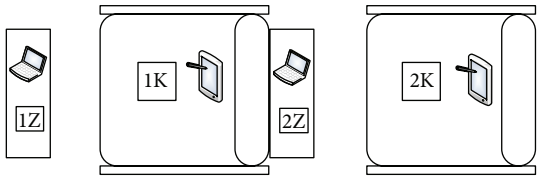

Figure 3: Position of table and seat back.

Table 1: The path loss values of 16th–20th rows dB.

Row	A	B	C	D	E
16Z	66.68	64.6	65.93	63.95	65.27
16K	64.03	62.53	60.83	62.9	62.75
17Z	65.61	65.02	64.49	62.81	63.55
17K	63.65	64.81	61.65	61.43	65.37
18Z	63	64.46	62.42	64.91	63.51
18K	62.01	62.2	62.16	61.03	62.96
19Z	63.84	63.33	63.31	64.83	65.47
19K	64.87	63.44	60.8	63.18	61.81
20Z	63.71	64.46	62.79	64.09	66.93
20K	61.58	64.09	59.53	60.48	66.06

As the measurements are carried out only in economy class, the 4th–25th rows are renumbered as row 1 to row 22 to facilitate the presentations. Thus only A, B, C, D, and E of row 1 to row 22 are considered. The renumbered rows are shown in Figure 2.

Besides, we define K to present the scenario of seat back and Z for tables behind seat back. Thus, for example, 1K means the back of the seat of first row, and 1Z means table of first row. Thus, there are 220 data points in total. The position of table and seat back is shown in Figure 3.

For example, the path loss values of 16th–20th rows are listed in Table 1.

3. The Traditional Surface Fitting Method for Path Loss Forecasting

The prediction of the path loss uses the method of fitting usually. In order to compare with the SVM prediction, the B-spline surface fitting method was adopted [14]. Firstly, we loaded cabin path loss values as input data to Matlab, as shown in Figure 4.

We removed some points which need to be predicted and got the fitting surface using the B-spline surface fitting method, as shown in Figure 5.

The comparison of the true values and the prediction values of the path loss values of the removed points is listed in Table 2, as well as the error analysis.

4. SVM-Based Path Loss Forecasting

4.1. The SVM-Based Path Loss Forecasting Model. The statistical learning theory (SLT) [15] is professional on the area of the machine learning, especially for the small sample. The linear regression is the basic idea of SVM. However, the linear regression is not suitable for some complex problems, so the linear SVM should be extended to the nonlinear SVM. Through the nonlinear regression, we can get the regression decision function. The K in the regression decision function is called the kernel function, which is very important. Different kernel functions will lead to different kinds of SVM algorithm.

4.1.1. The Linear Regression of the SVM. Assume the training sample set (x_i, y_i), $i = 1, \ldots, l$, $x_i \in R^n$ is an n-dimension input vector, and $y_i \in R^n$ is the output vector. Then the linear regression problem can be converted to the optimal problem below:

$$\begin{aligned} &\min \ \frac{1}{2}\|\omega\|^2 \\ &\text{s.t.} \ \left|\omega \cdot x_i + b - y_i\right| \le \varepsilon, \quad i = 1, \ldots, l, \end{aligned} \tag{7}$$

where ω is the vector of weight, $\omega \in R^n$, and b is the intercept, $b \in R$. As there may be some estimating errors, we introduce a parameter C and two slack variables ξ_i, ξ_i^*. Then the optimal problem above can be modified as follows:

$$\begin{aligned} &\min \ \left\{\frac{1}{2}\|\omega\|^2 + C\sum_i^l (\xi_i + \xi_i^*)\right\} \\ &\text{s.t.} \ \left|\omega \cdot x_i + b - y_i\right| \le \xi_i^* + \varepsilon \\ &y_i - (\omega \cdot x_i) - b \le \xi_i^* + \varepsilon \\ &\xi_i, \xi_i^* \ge 0, \quad i = 1, \ldots, l. \end{aligned} \tag{8}$$

Establish the Lagrange function and solve it under the KKT conditions. The dual problem of the original one is as follows:

$$\begin{aligned} \min \ &\left\{\frac{1}{2}\sum_{i,j=1}^l (\alpha_i^* - \alpha_i)(\alpha_j^* - \alpha_j)(x_i \cdot x_j)\right. \\ &\left. +\varepsilon\sum_i^l (\alpha_i^* + \alpha_i) - \sum_i^l y_i (\alpha_i^* - \alpha_i)\right\} \end{aligned} \tag{9}$$

$$\text{s.t.} \ \sum_i^l (\alpha_i - \alpha_i^*) = 0$$

$$0 \le \alpha_i, \quad \alpha_i^* \le C, \quad i = 1, \ldots, l.$$

At last, the regression decision function is as follows:

$$f(x) = \sum_{i}^{l} (\alpha_i - \alpha_i^*)(x_i \cdot x) + b. \quad (10)$$

4.1.2. The Nonlinear Regression. When the dataset cannot be linearly regressed, we can transform the original data into a high dimension feature space using a nonlinear mapping $\varphi(x)$, where we can carry out the linear regression. By defining the kernel function of the inner product of the high dimension feature space $K(x_i, y_i) = \varphi(x_i)\varphi(y_i)$, the inner product of a variable in the high dimension space can be obtained by operating in the original space through the kernel function:

$$\min \left\{ \frac{1}{2} \sum_{i,j=1}^{l} (\alpha_i^* - \alpha_i)(\alpha_j^* - \alpha_j) K(x_i \cdot x_j) + \varepsilon \sum_{i}^{l} (\alpha_i^* + \alpha_i) - \sum_{i}^{l} y_i (\alpha_i^* - \alpha_i) \right\} \quad (11)$$

$$\text{s.t.} \sum_{i}^{l} (\alpha_i - \alpha_i^*) = 0$$

$$0 \le \alpha_i, \quad \alpha_i^* \le C, \quad i = 1, \ldots, l.$$

At last, the regression decision function is as follows:

$$f(x) = \sum_{i}^{l} (\alpha_i - \alpha_i^*) K(x_i \cdot x) + b. \quad (12)$$

4.1.3. The Selection of the Kernel Function. Nowadays, the widely used kernel functions include the linear function, the polynomial kernel function, the Gauss radial basis kernel function, and the Sigmoid kernel function. The performance of the SVM has no relationship with the selection of the different types of the kernel function but has a strong relationship with the parameters in the kernel function. Nevertheless, we could select a good type of the kernel functions in order to reduce the calculation complexity.

As for the polynomial kernel function (the linear kernel function is a special case of the polynomial kernel function), when the eigenspace has a high dimension, the calculation amount could be huge, and what is even worse, we cannot obtain any correct solution under some certain situations. However, the Gauss radial basis kernel function can overcome similar problems. Furthermore, the selection of Gauss kernel function is connotative; that is, every support vector would produce a local Gauss function which is centered by the vector itself. We can find the global width of the basis function by structural risk minimization principle. As stated above, we take the Gauss radial basis kernel function in the following study.

4.2. The Choice of Input and Output Variables. We randomly select 5 rows (such as 16 to 20 rows), where only table data (Z) of the seats B and D are treated as unknown data (10 groups totally). We use SVM model to forecast these 10 groups of unknown data, in order to verify the accuracy of the SVM prediction model. The sample data of BCD is selected the reminder 30 rows (from 1K to 15Z and from 21K to 22Z). For one certain point, the surrounding eight points path

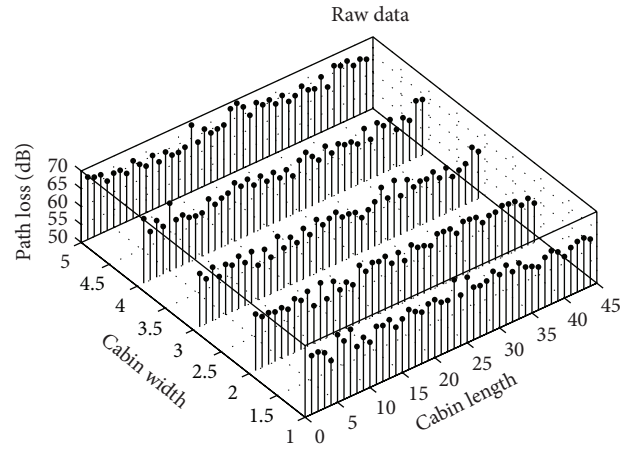

Figure 4: Raw data.

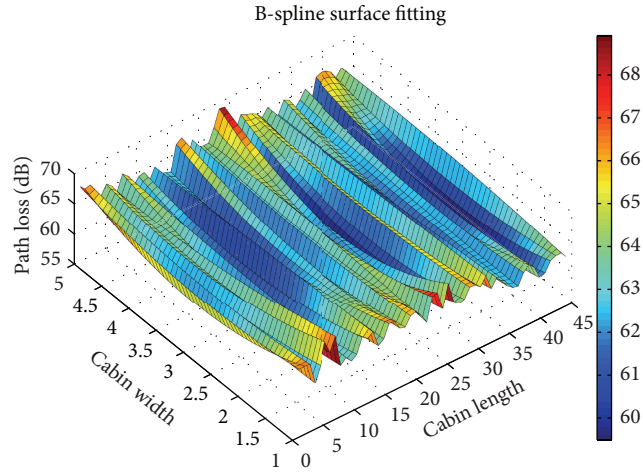

Figure 5: B-spline surface fitting.

Table 2: The error analysis of B-spline surface fitting dB.

Point	True value	Fitted value	Absolute error	Relative error
16ZB	64.6	66.14	1.54	2.38%
16ZD	63.95	65.45	1.5	2.35%
17ZB	65.02	64.58	0.44	0.68%
17ZD	62.81	63.49	0.68	1.08%
18ZB	64.46	62.36	2.1	3.26%
18ZD	64.91	62.47	2.44	3.76%
19ZB	63.33	63.18	0.15	0.24%
19ZD	64.83	63.71	1.12	1.73%
20ZB	64.46	62.75	1.71	2.65%
20ZD	64.09	63.79	0.3	0.47%

The average of the relative error using B-spline surface fitting is 1.86%.

Table 3: An example of input and output variables in SVM model dB.

Input data								Output data
66.39	65.77	64.91	62.58	65.01	64.51	65.5	66.57	64.26
(1ZA)	(1ZB)	(1ZC)	(1KC)	(2ZC)	(2ZB)	(2ZA)	(1KA)	(1KB)
65.77	64.91	68.01	63.6	65.83	65.01	64.51	64.26	62.58
(1ZB)	(1ZC)	(1ZD)	(1KD)	(2ZD)	(2ZC)	(2ZB)	(1KB)	(1KC)
64.91	68.01	67.44	66.61	66.42	65.83	65.01	62.58	63.6
(1ZC)	(1ZD)	(1ZE)	(1KE)	(2ZE)	(2ZD)	(2ZC)	(1KC)	(1KD)

Table 4: The error analysis of the 45 groups back of chairs training dB.

Point	True value	Fitted value	Absolute error	Relative error
16ZB	64.6	62.48	2.12	3.28%
16ZD	63.95	61.92	2.03	3.17%
17ZB	65.02	62.13	2.89	4.44%
17ZD	62.81	61.81	1	1.59%
18ZB	64.46	62.56	1.9	2.95%
18ZD	64.91	61.83	3.08	4.75%
19ZB	63.33	62.03	1.3	2.05%
19ZD	64.83	61.77	3.06	4.72%
20ZB	64.46	62.56	1.9	2.95%
20ZD	64.09	61.63	2.46	3.84%

Table 5: The error analysis of the 45 groups table of chairs training dB.

Point	True value	Fitted value	Absolute error	Relative error
16ZB	64.6	65.12	0.52	0.80%
16ZD	63.95	64.57	0.62	0.97%
17ZB	65.02	64.75	0.27	0.42%
17ZD	62.81	64.01	1.2	1.91%
18ZB	64.46	64.29	0.17	0.26%
18ZD	64.91	63.7	1.21	1.86%
19ZB	63.33	64.35	1.02	1.61%
19ZD	64.83	64.16	0.67	1.03%
20ZB	64.46	64.46	0	0%
20ZD	64.09	63.88	0.21	0.33%

loss values are selected as the eight input variables x_i, $i = 1, 2, \ldots, 8$, and the path loss value of this point is supposed as the output variables y. The ninety sets of data included forty-five sets of seat back data and forty-five sets of table data. The first 8 values of each line are input variables; the last data is the output variable. Examples of the path loss samples selected as the input data and the output data in SVM model are listed in Table 3.

4.3. Path Loss Prediction Using SVM-Based Model in Cabin

4.3.1. Case 1: Training Table Data Using Seat Back Data. Firstly, the training samples of the forty-five back data are selected from ninety sets. The data of forty-five groups are trained using SVM. The unknown data of row 16 to row 20 are predicted using the trained model. In order to verify the validity of the model, the error analysis is caculated for the real value and the predictive value, such as absolute error and relative error. The result is described in Table 4. The relative error in the table refers to the ratio of the real value and absolute error value.

We average the relative error in Table 4 and conclude that the average relative error predicted is 3.37%, which shows that the forecast is not very accurate using the samples of back of chair to train the table of chairs.

4.3.2. Case 2: Training Table Data Using Table Data. Then we select the rest of the 45 groups of table samples to train the model and send the 45 groups of data into SVM for training. We still forecast the 10 points mentioned above. The result is described in Table 5.

The average relative error predicted is 0.92%. The conclusion is that when we use the samples of the tables to train, as the training samples and the predicted samples share more relevance, which means that their channel environments are more similar, the model is more accurate.

4.3.3. Case 3: Training Table Data Using Both Seat Back and Table Data. Finally, we take all the 90 datasets, including samples on back of the chair and the table, into the SVM model for training. We forecast the 10 points mentioned above. The result is described in Table 6.

The average relative error predicted is 1.02%. It can be concluded that increasing training samples, which share less relevance with the predicted samples, makes no contribution to the accuracy of the prediction model.

5. Further Discussion

It can be concluded that the accuracy forecasted by SVM is increased greatly compared with the accuracy predicted by surface fitting. The relative average forecast error of SVM can reach 0.92% in Case 2. The relative average forecast error of surface fitting is 1.86% in this study, using the same measurement data. The accuracy of surface fitting and SVM fitting is compared in Figure 6.

For the surface fitting method, the plane is fitting of surface of these points, with smooth surface, connected from fitting surface to find needed points. The cabin environment of plane is very complex with a lot of seats, so the shadow

Table 6: The error analysis of all the 90 groups training dB.

Point	True value	Fitted value	Absolute error	Relative error
16ZB	64.6	65.14	0.54	0.84%
16ZD	63.95	64.95	1	1.56%
17ZB	65.02	64.34	0.68	1.05%
17ZD	62.81	63.92	1.11	1.77%
18ZB	64.46	63.94	0.52	0.81%
18ZD	64.91	63.48	1.43	2.20%
19ZB	63.33	63.81	0.48	0.76%
19ZD	64.83	64.38	0.45	0.69%
20ZB	64.46	64.43	0.03	0.05%
20ZD	64.09	64.37	0.28	0.44%

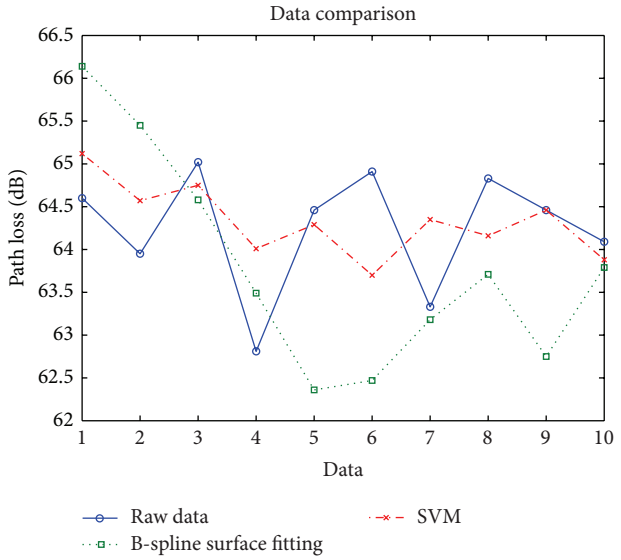

Figure 6: Data Comparasion.

fading will affect the signal strength greatly. However, most things in cabin are stable, so it is very suitable to forecast using SVM. The environment information included in the SVM training data can avoid the influence of shadow fading on predicting effectively.

It can also be concluded that the more relevance of the training samples and the predicted samples can improve the accuracy of the prediction model. Besides, more samples, which share less relevance with the predicted samples, make no contribution to the accuracy in statistical aspect.

One of the purposes of this paper is to reduce the amount of measurements. We need to reduce the measurement activities as far as possible and predict the unknown point using SVM-based model at an acceptable error level.

6. Conclusion

Although path loss can be obtained via theoretical prediction or field measurement, the method of Computational Electromagnetic and a lot of measurements without changing the cabin environment are very difficult to proceed, because the cabin is a big and complex space. The principle challenges are to simplify the complicate measurement and to improve the accuracy of prediction of the path loss. In this paper, an SVM-based path loss prediction method was first proposed to overcome the measurement challenges in complex and big cabin environment. We selected the path loss values around the predicted points as the input data of the prediction model and used the trained model to predict points not been measured. The path loss prediction results demonstrated that the proposed SVM-based prediction method is effective and accurate compared to the surface fitting method. The relevance of the training samples and the predicted samples can affect the accuracy of the prediction model. The proposed SVM-based path loss prediction method can forecast the points inconvenient to be measured, which can reduce the amount of measurement and provide supplement information in channel modeling.

Acknowledgments

This work was supported by the National Science and Technology Major Project of the Ministry of Science and Technology of China (Grant no. 2009ZX03007-003), the National High Technology Research and Development Program of China (Grant no. 2009AA011507), and the National Natural Science Foundation of China (Grant no. 61101223). The authors would like to thank Tsinghua University for providing the measurement data. The first author also would like to thank Associate Professor Yang Jinsheng and the project team members Mao Xiangfang and Wu Xuzhao for the helpful discussion.

References

[1] N. R. Díaz and J. E. J. Esquitino, "Wideband channel characterization for wireless communications inside a short haul aircraft," in *Proceedings of the IEEE 59th Vehicular Technology Conference*, pp. 223–228, Milan, Italy, May 2004.

[2] S. Chiu, J. Chuang, and D. G. Michelson, "Characterization of UWB channel impulse responses within the passenger cabin of a boeing 737-200 aircraft," *IEEE Transactions on Antennas and Propagation*, vol. 58, no. 3, pp. 935–945, 2010.

[3] K. Chetcuti, C. J. Debono, R. A. Farrugia, and S. Bruillot, "Wireless propagation modelling inside a business jet," in *Proceedings of the IEEE Eurocon (EUROCON '09)*, pp. 1644–1649, St.-Petersburg, Russia, May 2009.

[4] J. Jemai, R. Piesiewicz, R. Geise et al., "UWB channel modeling within an aircraft cabin," in *Proceedings of the IEEE International Conference on Ultra-Wideband, ICUWB 2008*, pp. 5–8, Hannover, Germany, September 2008.

[5] J. Chuang, N. Xin, H. Huang, S. Chiu, and D. G. Michelson, "UWB radiowave propagation within the passenger cabin of a boeing 737-200 aircraft," in *Proceedings of the IEEE 65th Vehicular Technology Conference*, pp. 496–500, Dublin, Ireland, April 2007.

[6] C. Cerasoli, "RF propagation in tunnel enviroments," in *Proceedings of the IEEE Military Communications Conference (OtLCOM '04)*, pp. 363–369, Monterey, Calif, USA, November 2004.

[7] E. Perrin, F. Tristant, S. Gouverneur et al., "Study of electric field radiated by wifi sources inside an aircraft—3D computations and real tests," in *Proceedings of the IEEE International Symposium on Electromagnetic Compatibility (EMC '08)*, pp. 1–5, Hamburg, Germany, September 2008.

[8] A. J. Smola and B. Schölkopf, "A tutorial on support vector regression," *Statistics and Computing*, vol. 14, no. 3, pp. 199–222, 2004.

[9] Z. Xiang, X. W. Liu, and R. C. Shangguan, "Research on the channel prediction algorithm of multiwavelet combined with support vector machines based on FPGA," in *Proceedings of the 6th International Conference on Natural Computation (ICNC '10)*, pp. 3614–3618, Yantai, Shandong, China, August 2010.

[10] J. P. Zhang, Y. N. Zhuo, and Y. Zhao, "Mobile location based on SVM In MIMO communication systems," in *Proceedings of the International Conference on Information, Networking and Automation (ICINA '10)*, pp. V2-360–V2-363, Kunming, China, October 2010.

[11] Y. H. Rui, Y. Zhang, S. J. Liu, and S. D. Zhou, "3.52 GHz MIMO radio channel sounder," in *Proceedings of the International Conference on Communications, Circuits and Systems (ICCCAS '08)*, pp. 79–83, Fujian, China, May 2008.

[12] X. W. Hu, Y. Zhang, Y. Z. Jia, S. D. Zhou, and L. M. Xiao, "Power coverage and fading characteristics of indoor distributed antenna systems," in *Proceedings of the 4th International Conference on Communications and Networking in China (CHINACOM '09)*, pp. 1066–1069, Xi'an, China, August 2009.

[13] C. H. Zhuo, S. J. Liu, Y. Zhang, Y. H. Rui, and S. D. Zhou, "A simple broadband MIMO channel sounder prototype," in *Proceedings of the International Conference on Wireless, Mobile and Multimedia Networks*, pp. 1–4, Hangzhou, China, 2006.

[14] Y. L. Hu and M. M. Li, "Surface fitting by splines using matlab," *Journal of Yunnan University for Nationalities*, vol. 14, no. 2, pp. 168–171, 2005.

[15] V. N. Vapnik, "An overview of statistical learning theory," *IEEE Transactions on Neural Networks*, vol. 10, no. 5, pp. 988–999, 1999.